

# Multi-Label Knowledge Distillation

Penghui Yang<sup>1,2\*</sup>, Ming-Kun Xie<sup>1,2\*</sup>, Chen-Chen Zong<sup>1,2</sup>, Lei Feng<sup>3</sup>,  
Gang Niu<sup>4</sup>, Masashi Sugiyama<sup>4,5</sup>, Sheng-Jun Huang<sup>1,2†</sup>

<sup>1</sup>College of Computer Science and Technology, Nanjing University of Aeronautics and Astronautics,

<sup>2</sup>MIIT Key Laboratory of Pattern Analysis and Machine Intelligence, Nanjing, China

<sup>3</sup>School of Computer Science and Engineering, Nanyang Technological University, Singapore

<sup>4</sup>RIKEN Center for Advanced Intelligence Project, <sup>5</sup>The University of Tokyo, Tokyo, Japan

phyang.cs@gmail.com, mkxie@nuaa.edu.cn, chencz@nuaa.edu.cn, lfengqag@gmail.com,

gang.niu.ml@gmail.com, sugi@k.u-tokyo.ac.jp, huangsj@nuaa.edu.cn

## Abstract

Existing knowledge distillation methods typically work by imparting the knowledge of output logits or intermediate feature maps from the teacher network to the student network, which is very successful in multi-class single-label learning. However, these methods can hardly be extended to the multi-label learning scenario, where each instance is associated with multiple semantic labels, because the prediction probabilities do not sum to one and feature maps of the whole example may ignore minor classes in such a scenario. In this paper, we propose a novel multi-label knowledge distillation method. On one hand, it exploits the informative semantic knowledge from the logits by dividing the multi-label learning problem into a set of binary classification problems; on the other hand, it enhances the distinctiveness of the learned feature representations by leveraging the structural information of label-wise embeddings. Experimental results on multiple benchmark datasets validate that the proposed method can avoid knowledge counteraction among labels, thus achieving superior performance against diverse comparing methods. Our code is available at: <https://github.com/penghui-yang/L2D>.

## 1. Introduction

Multi-label learning (MLL) addresses problems where each instance is assigned with multiple class labels simultaneously [40]. For example, as shown in Figure 1, an image of a street scene may be annotated with labels *bus*, *car* and *person*. To learn the complex object-label mapping, there is always necessity of training large models to obtain desirable performance in MLL. While the remarkable successes

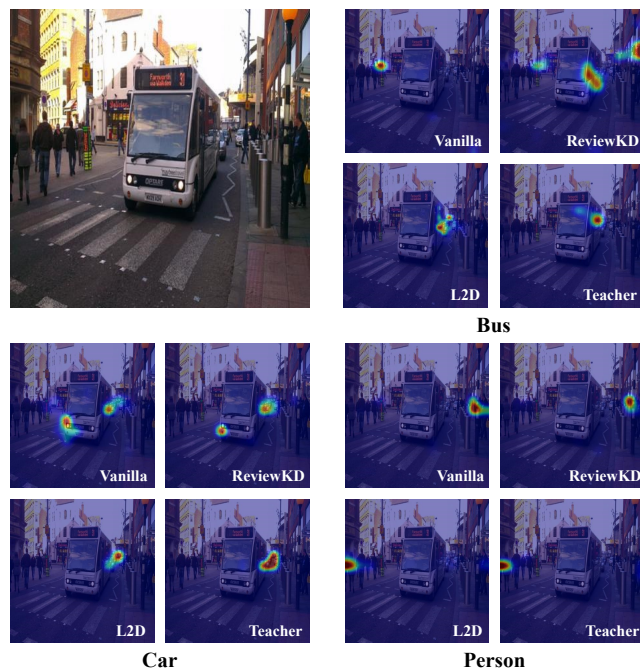


Figure 1. Visualization of attention maps on different classes. We compare our method with the following three baselines: 1) Vanilla: the student trained without distillation; 2) ReviewKD [1]: a feature-based method that achieves the state-of-the-art performance; 3) Teacher: the pretrained model used in distillation. It can be observed that: on the classes *bus* and *car*, L2D captures semantic objects more precisely than the conventional KD method; on the class *person*, although all of the methods focus on people, only our method focuses on the same person as the teacher, which validates that L2D can distill the “dark” knowledge [32] from the teacher more effectively. The backbones of the teacher and student models are respectively ResNet-101 and ResNet-34. More visualization of attention maps can be found in Appendix.

have been made in MLL through the training of deep neural networks (DNNs) [17, 27], it is hard to deploy these large

\*Both authors contributed equally to this research.

†Correspondence to: Sheng-Jun Huang (huangsj@nuaa.edu.cn).

models on lightweight terminals, *e.g.*, mobile phones, under the constraint of computational resource or requirement of short inference time.

To mitigate this issue, knowledge distillation (KD) [12] is needed which aims to improve the performance of a small network (also known as the “student”) by requiring the knowledge from a large network (also known as the “teacher”) to guide the training of the student network. Typical KD methods focus on the multi-class classification, and can be roughly divided into two categories: logits-based methods and feature-based methods. The former minimizes the difference between logits of the teacher model and the student model [12, 42], while the latter distills knowledge from feature maps of intermediate layers [23, 33, 1].

Although KD has been proven to be effective for improving the performance of the student network in single-label classification, it is still a challenging problem to directly extend existing KD methods to solve multi-label knowledge distillation (MLKD) problems. Specifically, logits-based methods often obtain the predicted probabilities based on the softmax function; this function is not suitable for MLKD, because the sum of predicted probabilities may not equal one in MLL. Feature-based methods often perform KD based on the feature maps of a whole image with multiple semantics, which makes the model focus on the major objects while neglect minor objects. For example, in Figure 1, Vanilla and ReviewKD wrongly focused on the *bus* when the model queried the label *car*. Such a phenomenon would cause the model to obtain sub-optimal even undesirable distillation performance.

Recently, several attempts have been made to utilize KD techniques for improving the performance of MLL [18, 35, 30]. There are mainly two differences between these works and our work. Firstly, these methods often required specifically-designed network architectures [18, 30] or training strategies [35] to train the teacher and student models, while our method focuses on studying MLKD in general scenarios without any extra requirement. Secondly, unlike the previous methods utilized KD as an auxiliary technique to improve the performance of MLL, our goal is to develop a tailored approach for MLKD. As a result, previous methods were mainly compared with MLL methods in their original papers, we evaluate the KD performance of our method by comparing it with state-of-the-art KD methods.

In this paper, to perform MLKD, we propose a new method consisting of multi-label logits distillation and label-wise embedding distillation (L2D for short). Specifically, to exploit informative semantic knowledge compressed in the logits, L2D employs the one-versus-all reduction strategy to obtain a set of binary classification problems and perform logits distillation for each one. To enhance the distinctiveness of learned feature representations,

L2D encourages the student model to maintain a consistent structure of intra-class and intra-instance (inter-class) label-wise embeddings with the teacher model. By leveraging the structural information of the teacher model, these two structural consistencies respectively enhance the compactness of intra-class embeddings and dispersion of inter-class embeddings for the student model. Both of these two components lead L2D to achieve better distillation performance than conventional KD methods as shown in Figure 1.

Our main contributions can be summarized as follows:

- A general framework called MLKD is proposed. To our best knowledge, the framework is the first study specially designed for knowledge distillation in the multi-label learning scenario.
- A new approach for MLKD called L2D is proposed. It performs multi-label logits distillation and label-wise embedding distillation simultaneously. The former provides informative semantic knowledge while the latter encourages the student model to learn more distinctive feature representations.
- Extensive experimental results on benchmark datasets demonstrate the effectiveness of our proposed method.

## 2. Related Work

The concept of knowledge distillation (KD) proposed by Geoffrey Hinton *et al.* [12] defines a learning framework that transfers knowledge from a large teacher network to a small student network. Existing works can be roughly divided into two groups, *i.e.*, logits-based methods and feature-based methods. Logits-based methods mainly focus on designing effective distillation losses to distill knowledge from logits and softmax scores after logits. DML [41] introduces a mutual learning method to train both teachers and students simultaneously. TAKD [22] proposes a new architecture called “teacher assistant”, which is an intermediate-sized network bridging the gap between teachers and students. Besides, a recent study [42] proposes a novel logits-based method to reformulate the classical KD loss into two parts and achieves the state-of-the-art performance by adjusting weights for these two parts. Some other methods focus on distilling knowledge from intermediate feature layers. FitNet [28] is the first approach to distill knowledge from intermediate features by measuring the distance between feature maps. Attention transfer [38] achieves better performance than FitNet by distilling knowledge from the attention maps. PKT [24] measures the KL divergence between features by treating them as probability distributions. RKD [23] utilizes the relations among instances to guide the training process of the student model. CRD [33] incorporates contrastive learning into knowledge distillation. ReviewKD [1] proposes a review mechanism

which uses multiple layers in the teacher to supervise one layer in the student. ITRD [21] aims to maximize the correlation and mutual information between the students and teachers representations.

Multi-label learning has increasingly attracted a lot of interest recently. Existing solutions for solving MLL problems can be categorized into three directions. The first type attempts to design novel loss functions for tackling the intrinsic positive-negative imbalance issue in multi-label classification tasks. For example, ASL [26] uses different weights to re-weight positive and negative examples for the balanced training. The second type focuses on modeling the label correlations, which provides prior knowledge for multi-label classification. Among them, MLGCN [3] is a representative method that employs a graph convolutional network to model correlation matrix. CADM [2] constructs a similar graph based on class-aware maps. To handle the multiple semantic objects contained in an image, the last type of methods aims to locate areas of interest related to semantic labels by using attention techniques. Among them, C-Tran [15] first utilizes the transformer to retrieve embeddings from visual features for each label. Query2Label [17] uses several stacked transformer encoders to identify interesting areas. ML-Decoder [27] simplifies transformer encoders in Query2Label. ADDS [36] introduces encoders from CLIP [25] in order to get better textual and visual embedding inputs to the classification head. In addition, ADDS adds a multi-head cross-attention layer and a skipping connection from the query input to the query output based on ML-Decoder.

Several previous studies have applied KD techniques to improve the performance of MLL. For example, Yongcheng Liu *et al.* [18] and Jiazhi Xu *et al.* [35] simply minimized mean squared error (MSE) loss between teacher logits and student logits. Liangchen Song *et al.* [30] designed a partial softmax function by combining a positive label with all other negative labels. Then, the conventional KD loss can be computed for each positive label. Although these methods made the pioneering attempts of combining KD and MLL, they cannot be directly applied general MLKD scenarios, and also fail to evaluate their KD performance by comparing with KD methods.

### 3. The Proposed Approach

Let  $\mathbf{x} \in \mathcal{X}$  be an instance and  $\mathbf{y} \in \mathcal{Y}$  be its corresponding label vector, where  $\mathcal{X} \subset \mathbb{R}^d$  is the input space with  $d$  dimensions and  $\mathcal{Y} \subset \{0, 1\}^q$  is the target space with  $q$  class labels. We further use  $y_j$  to denote the  $j$ -th component of  $\mathbf{y}$ . For a given instance  $\mathbf{x}$ ,  $y_j = 1$  indicates the  $j$ -th label is relevant to the instance;  $y_j = 0$ , otherwise. In multi-label learning, each instance may be assigned with more than one label, which means  $\sum_{j=1}^q \mathbb{I}(y_j = 1) \geq 1$ , where  $\mathbb{I}(\cdot)$  is the indicator function. We also denote by  $[q]$  the integer set

$\{1, 2, \dots, q\}$ .

In this paper, we use a classification model consisting of three components, *i.e.*, a visual backbone  $f$ , which extracts a feature map  $f(\mathbf{x})$  for the input  $\mathbf{x}$ , a label-wise embedding encoder  $g$  [15, 17], which produces a label-wise embedding  $e_k = g_k(f(\mathbf{x}))$  with respect to the  $k$ -th class based on the feature map  $f(\mathbf{x})$ , and a multi-label classifier  $h$ , which predicts multi-label probabilities  $\hat{\mathbf{y}} = [\sigma(h_1(e_1)), \sigma(h_2(e_2)), \dots, \sigma(h_q(e_q))]$ , where  $\sigma(\cdot)$  denotes the sigmoid function. It is noteworthy that the used model is very general, which can be built by equipping commonly used backbones, *e.g.*, ResNet [11], with a label-wise embedding encoder  $g$ . For the notations mentioned above, we use the superscripts  $\mathcal{T}$  (or  $\mathcal{S}$ ) to denote the teacher (or student) model. For example, we use  $e_k^{\mathcal{T}}$  and  $e_k^{\mathcal{S}}$  to denote the label-wise embeddings for teacher and student models.

In multi-label learning, a popular method is to employ the one-versus-all reduction strategy to transform the original task into multiple binary problems. Among the various loss functions, the most commonly used one is the binary cross entropy (BCE) loss. Specifically, given a batch of examples  $\{(\mathbf{x}_i, \mathbf{y}_i)\}_{i=1}^b$  and the predicted probabilities  $\hat{\mathbf{y}}$ , the BCE loss can be defined as follows:

$$\mathcal{L}_{\text{BCE}} = -\frac{1}{b} \sum_{i=1}^b \sum_{k=1}^q y_{ik} \log(\hat{y}_{ik}) + (1 - y_{ik}) \log(1 - \hat{y}_{ik}). \quad (1)$$

Figure 2 illustrates the distillation process of the proposed L2D framework. For a batch of training examples, we feed them into the teacher/student model to obtain the label-wise embeddings and predicted probabilities. In order to train the student model, besides the BCE loss, we design the following two distillation losses: 1) multi-label logits distillation loss  $\mathcal{L}_{\text{MLD}}$  to exploit informative semantic knowledge compressed in the logits, 2) label-wise embedding distillation loss  $\mathcal{L}_{\text{LED}}$  to leverage structural information for enhancing the distinctiveness of learned feature representations. The overall objective function can be presented as

$$\mathcal{L}_{\text{L2D}} = \mathcal{L}_{\text{BCE}} + \lambda_{\text{MLD}} \mathcal{L}_{\text{MLD}} + \lambda_{\text{LED}} \mathcal{L}_{\text{LED}}, \quad (2)$$

where  $\lambda_{\text{MLD}}$  and  $\lambda_{\text{LED}}$  are two balancing parameters.

#### 3.1. Multi-Label Logits Distillation

Traditional logits-based distillation normally minimizes the Kullback-Leibler (KL) divergence between the predicted probabilities, *i.e.*, the logits after the softmax function, of teacher and student model. However, the method cannot be directly applied to the MLL scenario, since it depends on a basic assumption that the predicted probabilities of all classes should sum to one, which hardly holds for MLL examples.

To mitigate this issue, inspired by the idea of one-versus-all reduction, we propose a multi-label logits distillation

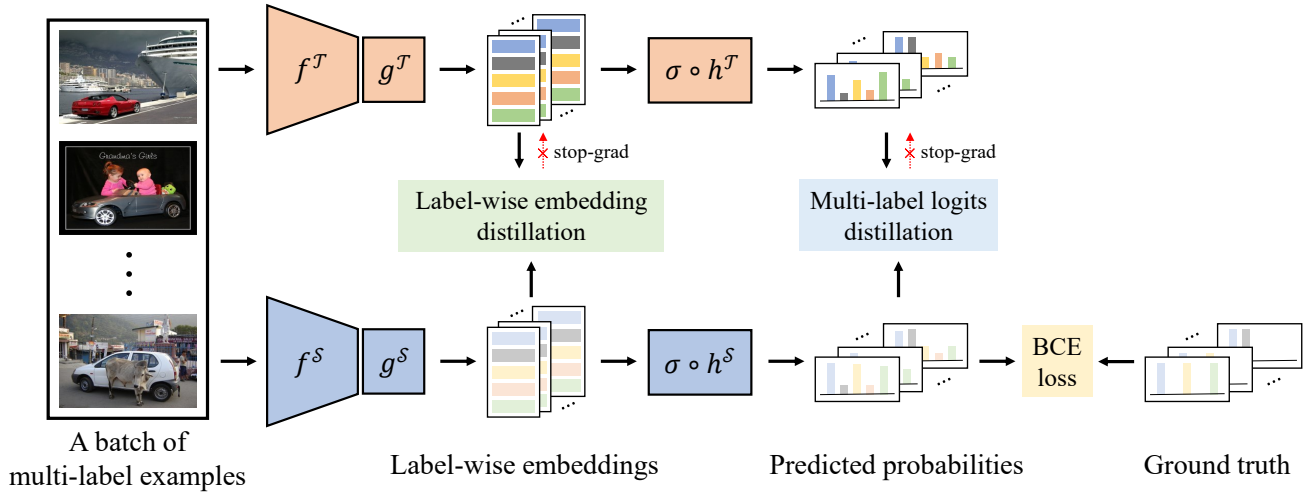


Figure 2. An illustration of the L2D framework. The framework simultaneously performs multi-label logits distillation and label-wise embedding distillation to improve the performance of the student model.

(MLD) loss, which decomposes the original multi-label task into multiple binary classification problems and minimizes the divergence between the binary predicted probabilities of two models. Formally, the MLD loss can be formulated as follows:

$$\mathcal{L}_{\text{MLD}} = \frac{1}{b} \sum_{i=1}^b \sum_{k=1}^q \mathcal{D}([\hat{y}_{ik}^T, 1 - \hat{y}_{ik}^T] \parallel [\hat{y}_{ik}^S, 1 - \hat{y}_{ik}^S]), \quad (3)$$

where  $[\cdot, \cdot]$  is an operator used to concatenate two scalars into a vector, and  $\mathcal{D}$  is a divergence function. The most common choice is the KL divergence  $\mathcal{D}_{\text{KL}}(P \parallel Q) = \sum_{x \in \mathcal{X}} P(x) \log \left( \frac{P(x)}{Q(x)} \right)$ , where  $P$  and  $Q$  are two different probability distributions. The MLD loss aims to improve the performance of student model by sufficiently exploiting informative knowledge from logits.

### 3.2. Label-wise Embedding Distillation

The MLD loss performs distillation on the predicted probabilities that can be regarded as a high-level representation, i.e., the final outputs of model. The knowledge distilled from the teacher model by only using the MLD loss would be insufficient to train a student model with desirable performance due to the limited information carried by the logits. To further strengthen the effectiveness of distillation, we design the label-wise embedding distillation (LED) loss, which aims to explore the structural knowledge from label-wise embeddings. The main idea is to capture two types of structural relations among label-wise embeddings: 1) class-aware label-wise embedding distillation (CD) loss  $\mathcal{L}_{\text{CD}}$ , which captures the structural relation between any two intra-class label-wise embeddings from different examples; 2) instance-aware label-wise embedding distillation (ID) loss  $\mathcal{L}_{\text{ID}}$ , which models the structural re-

lation between any two inter-class label-wise embeddings from the same example. In the following content, we introduce these two distillation losses in detail.

#### 3.2.1 Class-Aware Label-Wise Embedding Distillation

Class-aware label-wise embedding distillation aims to improve the distillation performance by exploiting the structural relations among intra-class label-wise embeddings. Generally, the same semantic objects from two different images often differ from each other by their individual characteristics, such as two cars with different colors and diverse styles (see the left side in Figure 3). Since our goal is to distinguish between *car* and other semantic classes instead of identifying different cars, these distinctiveness would be confusing information for the corresponding classification task. Due to the powerful learning capacity, the large model is able to capture the highly abstract semantic representations for each class label by neglecting the useless individual information. From the perspective of learned feature representations, as shown in the left side of Figure 3, the teacher model tends to obtain a more compact structure of intra-class label-wise embedding, which often leads to better classification performance. By transferring the structural knowledge from the teacher model to the student model, CD encourages the student model to enhance the compactness of intra-class label-wise embeddings, which can improve its classification performance.

For a batch of examples, let  $\{e_{ik}^T\}_{i=1}^b$  and  $\{e_{ik}^S\}_{i=1}^b$  respectively denote the intra-class label-wise embeddings with respect to class  $k \in [q]$  generated by the teacher and student models. Then, we can capture the structural relation between any two intra-class label-wise embeddings  $e_{ik}^T$  and

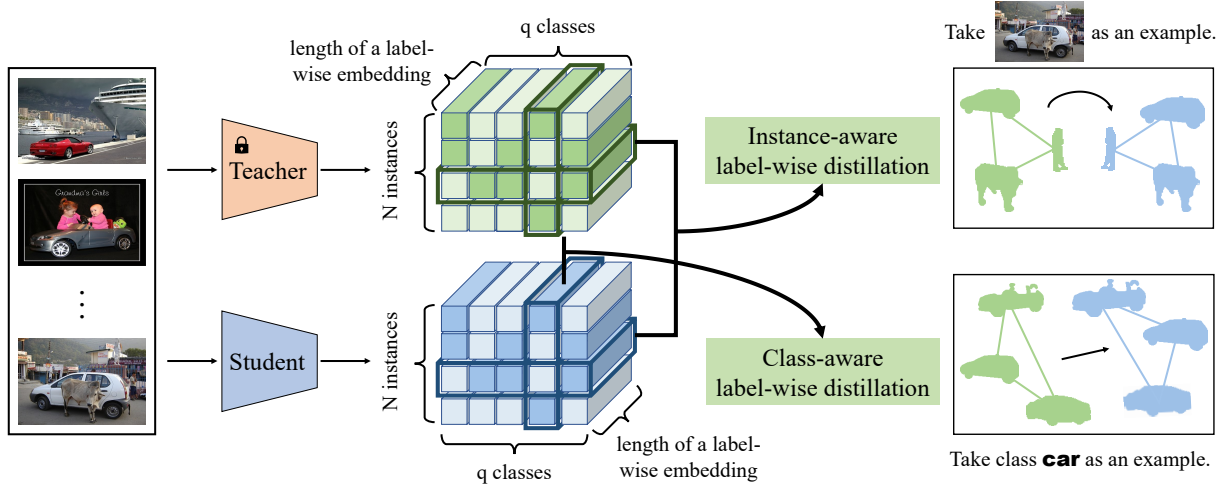


Figure 3. An illustration of class/instance-aware label-wise embedding distillation. Class-aware label-wise embedding distillation (CD) captures structural relations among intra-class label-wise embeddings from different examples, while instance-aware label-wise embedding distillation (ID) explores structural relations among intra-instance (inter-class) label-wise embeddings.

$e_{jk}^T$  by measuring their distance in the embedding space:

$$\phi_{CD}(e_{ik}^T, e_{jk}^T) = \begin{cases} \|e_{ik}^T - e_{jk}^T\|_2 & y_{ik} = 1, y_{jk} = 1, \\ 0 & \text{otherwise.} \end{cases} \quad (4)$$

It is worth to note that we only consider the structural relation between any two valid label-wise embeddings, *i.e.*, the embeddings with respect to positive labels. Similar to Eq.(4), for any two intra-class label-wise embeddings  $e_{ik}^S$  and  $e_{jk}^S$ , we can obtain the structural relation  $\phi_{CD}(e_{ik}^S, e_{jk}^S)$  for the student model.

By enforcing the teacher and student structural relations to maintain the consistency for each pair of intra-class label-wise embeddings, we can achieve the class-aware structural consistency as follows:

$$\mathcal{L}_{CD} = \sum_{k=1}^q \sum_{i,j \in [b]} \ell(\phi_{CD}(e_{ik}^T, e_{jk}^T), \phi_{CD}(e_{ik}^S, e_{jk}^S)), \quad (5)$$

where  $\ell$  is a function to measure the consistency between the teacher and student structural relations. In experiments, we use the following Huber loss function as a measurement:

$$\ell(a, b) = \begin{cases} \frac{1}{2}(a - b)^2 & |a - b| \leq 1, \\ |a - b| - \frac{1}{2} & \text{otherwise.} \end{cases} \quad (6)$$

where  $a$  and  $b$  are two different structural relations.

### 3.2.2 Instance-Aware Label-Wise Embedding Distillation

Instance-aware label-wise embedding distillation (ID) aims to improve the distillation performance by exploring the

structural relations among inter-class label-wise embeddings from the same image. Generally, one can hardly distinguish between two different semantic objects occurring in an image due to the high similarities they share. For example, in the upper left corner of Figure 3, an image annotated with both *sky* and *sea* makes it difficult to distinguish between the semantic objects, as they share the same color and similar texture. A feasible solution is to exploit other useful information, such as their spatial relation, *i.e.*, *sky* is always above *sea*. Due to the powerful learning capacity, the large model is able to distinguish between the similar semantic objects by exploiting such implicit supervised information. From the perspective of learned feature representations, as shown in the right side of 3, the teacher model tends to learn a dispersed structure of inter-class label-wise embedding, which is beneficial for improving its discrimination ability. By distilling the structural knowledge from the teacher model, ID enforces the student model to enhance the dispersion of inter-class label-wise embeddings, which can improve its discrimination ability.

For a given instance  $x_i$ , let  $\{e_{ik}^T\}_{k=1}^q$  and  $\{e_{ik}^S\}_{k=1}^q$  respectively denote the label-wise embeddings generated by teacher and student models. Then, we can capture the structural relation between any two inter-class label-wise embeddings  $e_{ik}^T$  and  $e_{il}^T$  by measuring their distance in the embedding space:

$$\phi_{ID}(e_{ik}^T, e_{il}^T) = \begin{cases} \|e_{ik}^T - e_{il}^T\|_2 & y_{ik} = 1, y_{il} = 1, \\ 0 & \text{otherwise.} \end{cases} \quad (7)$$

Note that in Eq.(7), we only consider the structural relation between any two valid label-wise embeddings, *i.e.*,

Table 1. Results on MS-COCO where teacher and student models are in the **same** architectures.

Teacher	RepVGG-A2			ResNet-101			WRN-101			Swin-S		
Student	RepVGG-A0			ResNet-34			WRN-50			Swin-T		
Metrics	mAP	OF1	CF1									
Teacher	72.71	74.11	68.63	73.62	73.89	68.61	74.70	75.56	70.73	81.70	80.48	77.12
Student	70.02	72.49	66.77	70.31	72.49	66.82	74.45	75.43	70.61	79.59	79.18	75.42
RKD	70.08	72.39	66.73	70.13	72.44	66.78	74.70	75.71	70.84	79.63	79.19	75.57
PKT	70.11	72.47	66.80	70.43	72.64	66.68	74.54	75.47	70.58	79.64	79.09	75.39
ReviewKD	70.00	72.35	66.82	70.39	72.62	66.76	74.03	75.29	70.36	79.81	79.18	75.55
MSE	70.26	72.54	66.99	70.54	72.75	66.85	74.53	75.60	70.71	79.67	79.20	75.52
PS	70.65	72.89	67.60	70.86	72.66	67.12	75.12	76.05	71.63	79.96	79.64	76.20
MLD	70.74	72.81	67.46	70.68	72.69	67.19	74.92	75.75	71.21	80.11	79.68	76.44
L2D	<b>72.81</b>	<b>74.59</b>	<b>69.49</b>	<b>72.87</b>	<b>74.45</b>	<b>69.43</b>	<b>76.61</b>	<b>77.08</b>	<b>72.79</b>	<b>81.59</b>	<b>81.03</b>	<b>77.86</b>

Table 2. Results on MS-COCO where teacher and student models are in the **different** architectures.

Teacher	ResNet-101			Swin-T			ResNet-101			Swin-T		
Student	RepVGG-A0			ResNet-34			MobileNet v2			MobileNet v2		
Metrics	mAP	OF1	CF1									
Teacher	73.62	73.89	68.61	79.43	78.77	75.07	73.62	73.89	68.61	79.43	78.77	75.07
Student	70.02	72.49	66.77	70.31	72.49	66.82	71.85	73.59	68.26	71.85	73.59	68.26
RKD	70.08	72.35	66.72	70.00	72.34	66.64	71.76	73.68	68.40	71.74	73.68	68.37
PKT	69.99	72.35	66.56	70.26	72.39	66.82	71.88	73.60	68.35	71.84	73.76	68.37
ReviewKD	70.00	72.33	66.62	70.29	72.39	66.58	71.92	73.73	68.48	71.73	73.71	68.36
MSE	70.07	72.50	66.85	70.33	72.57	66.72	71.91	73.68	68.28	71.80	73.74	68.38
PS	70.30	72.61	67.10	70.94	72.93	67.57	72.11	73.89	68.42	72.42	74.14	68.94
MLD	70.48	72.77	67.10	71.14	72.99	67.63	72.17	73.84	68.52	72.35	74.10	68.91
L2D	<b>72.14</b>	<b>74.08</b>	<b>68.78</b>	<b>73.42</b>	<b>74.97</b>	<b>70.20</b>	<b>73.24</b>	<b>74.85</b>	<b>69.72</b>	<b>74.21</b>	<b>75.72</b>	<b>70.87</b>

the embedding with respect to positive labels. Similar to Eq.(7), for any two inter-class label-wise embeddings  $e_{ik}^S$  and  $e_{il}^S$ , we can obtain the structural relation  $\phi_{ID}(e_{ik}^S, e_{il}^S)$  for the student model.

By encouraging the teacher and student model to maintain the consistent structure of intra-instance label-wise embeddings, we can minimize the following  $\mathcal{L}_{ID}$  loss to achieve the instance-aware structural consistency where  $\ell(\cdot)$  is Huber loss as defined in Eq.(6):

$$\mathcal{L}_{ID} = \sum_{i=1}^b \sum_{k,l \in [q]} \ell(\phi_{ID}(e_{ik}^T, e_{il}^T), \phi_{ID}(e_{ik}^S, e_{il}^S)). \quad (8)$$

Finally, the overall objective function of L2D (Eq.(2)) can be re-written as follows:

$$\mathcal{L}_{L2D} = \mathcal{L}_{BCE} + \lambda_{MLD} \mathcal{L}_{MLD} + \lambda_{CD} \mathcal{L}_{CD} + \lambda_{ID} \mathcal{L}_{ID}, \quad (9)$$

where  $\lambda_{MLD}$ ,  $\lambda_{CD}$  and  $\lambda_{ID}$  are all balancing parameters.

## 4. Experiments

**Datasets.** We perform experiments on three benchmark datasets Pascal VOC2007 [9] (VOC for short), MS-

COCO2014 [16] (MS-COCO for short) and NUS-WIDE [4]. VOC contains 5,011 images in the train-val set, and 4,952 images in the test set. It covers 20 common objects, with an average of 1.6 labels per image. MS-COCO contains 82,081 training images and 40,137 test images. It covers 80 common objects, with an average of 2.9 labels per image. NUS-WIDE contains 161,789 training images and 107,859 test images. It covers 81 visual concepts, with an average of 1.9 labels per image.

**Metrics.** Following existing works [40, 17, 31], we adopt the mean average precision (mAP) over all classes, overall F1-score (OF1) and average per-class F1-score (CF1) to evaluate the performance. We choose OF1 and CF1, since they consider both recall and precision and thus are more comprehensive.

**Comparing Methods.** To validate the proposed method, we compare it with the following sota KD methods: RKD [23], which captures the relations among instances to guide the training of the student model; PKT [24], which measures KL divergence between features by treating them as probability distributions; ReviewKD [1], which transfers

knowledge across different stages instead of just focusing on features in the same levels; as well as the modified KD techniques that have been applied to MLL: MSE [35], which minimizes the MSE loss between logits of teacher and student model; PS [30], which minimizes KL divergence of logits after a partial softmax function.

**Implementation Details.** We use the models pretrained on ImageNet [6] as the backbones. We resize the resolution of all images to  $224 \times 224$  and set the batch size as 64. For each training image, we adopt a weak augmentation consisting of random horizontal flipping and a strong augmentation consisting of Cutout [7] and RandAugment [5]. We use the Adam optimization method [14] to train the model for 80 epochs. The one-cycle policy is used with a maximal learning rate of 0.0001 and the weight decay [20] of 0.0001. For all experiments, we set  $\lambda_{MLD} = 10$ ,  $\lambda_{CD} = 100$ , and  $\lambda_{ID} = 1000$ . Parameter sensitivity analysis in Appendix shows that the performance of L2D are insensitive to all of our balancing parameters. For the comparing methods, we set their parameters as suggested in the original papers. Especially, for all feature-based methods, we just deploy them on the feature maps which is output from the visual backbone  $f$ . All the experiments are conducted on GeForce RTX 2080 GPUs. More details about the used models and implementation of the label-wise embedding encoder are attached in Appendix.

#### 4.1. Comparison Results

Table 1 and Table 2 report comparison results on MS-COCO with the same and different architectures of student and teacher models. From Table 1, it can be observed that: 1) Conventional feature-based distillation methods only achieve minor improvements in performance when compared with the student model (without distillation). This indicates these methods do not work in multi-label scenarios due to their disability to capture multiple semantics occurred in feature maps. 2) MLD can outperform conventional feature-based distillation methods in most cases, which indicates by performing one-versus-all reduction, the logits-based distillation can be adapted into multi-label knowledge distillation. 3) The proposed L2D significantly outperforms all other methods and achieves comparable performance with the teacher model. In particular, when WRN is used as the backbone, the performance of L2D is even better than that of teacher model. One possible reason is that L2D can effectively alleviate the over-fitting issue occurred to the teacher model. More results about reversed knowledge distillation where the Vanilla student model outperforms the teacher can be found in Appendix. From Table 2, we can see that compared with the same architecture, the performance gap between teacher and student model is larger for different architectures, which indicates the corresponding distillation task becomes harder. Our method sig-

Table 3. Comparison results of the comparing methods on VOC in terms of AP and mAP (%), where the backbones of teacher and student model are respectively ResNet-50 and ResNet-18. The best performance is highlighted in **red**, and second best performance is highlighted in **blue**.

Methods	Vanilla	RKD	PKT	MSE	MLD	L2D
bottle	57.18	<b>59.01</b>	57.29	58.26	58.32	<b>59.71</b>
pottedplant	67.43	67.01	66.16	68.02	<b>68.88</b>	<b>70.52</b>
chair	70.35	<b>71.31</b>	71.16	70.68	71.12	<b>74.77</b>
sofa	73.17	72.86	73.22	72.06	<b>73.77</b>	<b>75.01</b>
diningtable	76.14	76.90	76.89	77.93	<b>78.65</b>	<b>78.93</b>
cow	82.65	81.11	81.75	81.06	<b>84.60</b>	<b>83.87</b>
tvmonitor	82.30	81.70	81.95	82.36	<b>82.42</b>	<b>84.13</b>
bus	85.53	84.79	85.06	<b>86.03</b>	<b>86.41</b>	85.45
sheep	84.16	<b>84.77</b>	83.66	83.72	83.77	<b>85.67</b>
motorbike	88.38	<b>88.86</b>	88.73	88.30	88.58	<b>89.83</b>
dog	90.18	90.03	90.10	90.46	<b>90.78</b>	<b>90.60</b>
bird	90.65	<b>91.65</b>	91.31	90.60	91.02	<b>91.48</b>
bicycle	91.40	91.53	91.77	91.58	<b>91.92</b>	<b>91.90</b>
cat	90.67	<b>91.86</b>	91.83	91.07	91.63	<b>92.14</b>
boat	<b>92.54</b>	92.53	92.35	91.64	92.25	<b>92.57</b>
car	<b>92.72</b>	92.06	92.07	92.01	92.34	<b>93.40</b>
horse	94.22	93.97	93.12	94.05	<b>94.53</b>	<b>94.67</b>
person	95.73	95.88	95.80	95.69	<b>96.04</b>	<b>96.46</b>
train	96.09	<b>97.08</b>	96.99	<b>97.13</b>	96.97	96.81
aeroplane	97.27	97.00	97.09	97.10	<b>97.30</b>	<b>97.39</b>
mAP	84.01	84.18	83.86	84.23	<b>84.48</b>	<b>85.71</b>

Table 4. Ablation studies on MS-COCO.

MLD	CD	ID	mAP	OF1	CF1
			70.31	72.49	66.82
✓			70.68	72.69	67.19
✓	✓		71.91	73.74	68.76
✓		✓	71.79	73.62	68.43
✓	✓	✓	72.87	74.45	69.43

nificantly outperforms all the comparing methods by a significant margin in all cases. These results provide a strong empirical validation for the effectiveness of the proposed method.

Table 3 illustrates the performance of the proposed methods and other comparing methods on VOC in terms of AP and mAP. It is noteworthy that the performance is ranked in descending according to the performance of student model. From the figure, it can be observed that: 1) Our proposed L2D achieves the best performance and significantly outperforms the comparing methods in terms of mAP. 2) L2D consistently achieves superior performance to the comparing methods in most classes and the performance gap is large especially for classes that the student model achieves poor performance. This observation discloses that L2D improves the performance of hard classes by enhancing the distinctiveness of feature representations. These experimental results demonstrate the practical usefulness of the proposed method. More results on VOC and NUS-WIDE



Figure 4. Top-5 returned images with the query image. The returned results on the left are based on ReviewKD, while the results on the right are based on L2D. All results are sorted in the ascending order according to the distance from the query image. Red labels indicate that they are not included in the returned images’ labels, while green labels are shared by the query image and the returned one.

can be found in Appendix.

## 4.2. Ablation Study

In this section, to further analyze how the proposed method improves distillation performance, Table 4 reports results of ablation studies on MS-COCO (teacher: ResNet-101, student: ResNet-34). The first line in Table 4 reports the performance of student model without knowledge distillation. It can be observed that the distillation performance is improved slightly by only conducting multi-label logits distillation. Compared with MLD, label-wise embeddings distillation achieves the major improvement for the proposed method. It can be observed that by performing CD and ID, the mAP performance achieves 1.6% and 1.48% increments, respectively. Finally, we also examine the combination of these techniques. By incorporating these components together, the fusing method achieves the best performance and significantly outperforms each other method. These results demonstrate that all of three components are of great importance to the performance of the proposed L2D.

## 4.3. Performance on Image Retrieval

To further evaluate if our method can learn better representations, we conduct an image retrieval experiment. Specifically, we use the  $k$ -NN algorithm to perform content-based image retrieval, and choose the student model trained by ReviewKD as the baseline, which has achieved the best performance among all conventional KD methods. Figure 4 illustrates the top-5 images returned by both methods. The labels under each image are colored in green if they are shared by both the query image and the returned one, and otherwise in red. These images are sorted in the ascending order based on the distance to the query image in the representation space. From the figures, we can see that our method returns the images that match the query image better than ReviewKD. This indicates our approach can obtain better representations than conventional KD methods.

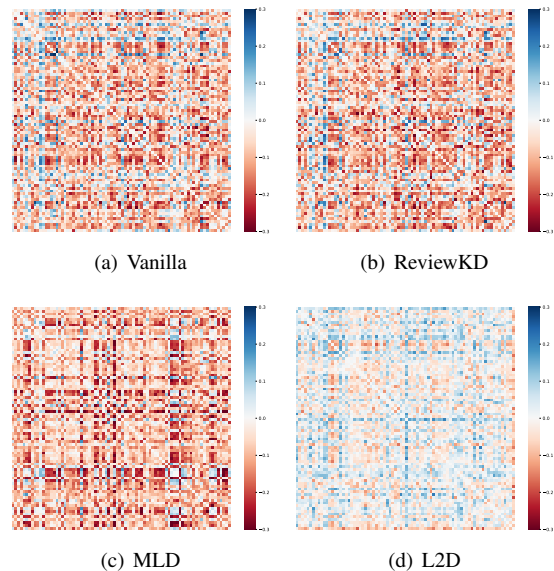


Figure 5. The differences between correlation matrices of student and teacher predicted probabilities on MS-COCO.

## 4.4. Distilling Inter-class Correlations

As discussed in the previous works [12], the conventional supervised learning losses, *e.g.*, BCE loss, often neglects the correlations among class predictions, which act as a foundational element in MLL. To validate whether the correlations can be captured by L2D effectively, Figure 5 illustrates the differences between correlation matrices of student and teacher predicted probabilities on MS-COCO. From the figure, it can be observed that: 1) The representative comparing method ReviewKD shows a large difference, which discloses that the conventional KD methods are ineffective to capture the correlations in multi-label scenarios. 2) MLD does not show a reduced difference, which indicates that the information of logits is not enough for capturing precise correlations. 3) L2D shows significant matching between the teacher and student correlations. By enhancing the distinctiveness of label-wise embeddings, L2D can obtain more correct predicted probabilities, leading to a more precise correlation estimation.

## 5. Conclusion

The paper studies the problem of multi-label knowledge distillation. In the proposed method, the multi-label logits distillation explores the informative semantic knowledge compressed in the teacher logits to obtain more semantic supervision. Furthermore, the label-wise embedding distillation exploits the structural knowledge from label-wise embeddings to learn more distinctive feature representations. Experimental results on benchmark datasets validate the effectiveness of the proposed method. In future, we plan to improve the performance of MLKD by exploiting other abundant structural information.

## Acknowledgement

Sheng-Jun Huang was supported by, the National Key R&D Program of China (2020AAA0107000), the Natural Science Foundation of Jiangsu Province of China (BK20222012, BK20211517), and NSFC (62222605). Lei Feng was supported by the Joint NTU-WeBank Research Centre on Fintech (Award No: NWJ-2021-005), Nanyang Technological University, Singapore, Chongqing Overseas Chinese Entrepreneurship and Innovation Support Program, Chongqing Artificial Intelligence Innovation Center, and CAAI-Huawei MindSpore Open Fund. Masashi Sugiyama was supported by JST CREST Grant Number JP-MJCR18A2.

## References

- [1] Pengguang Chen, Shu Liu, Hengshuang Zhao, and Jiaya Jia. Distilling knowledge via knowledge review. In *Proceedings of the IEEE/CVF Conference on Computer Vision and Pattern Recognition*, pages 5008–5017, 2021. 1, 2, 6
- [2] Zhao-Min Chen, Xiu-Shen Wei, Xin Jin, and Yanwen Guo. Multi-label image recognition with joint class-aware map disentangling and label correlation embedding. In *Proceedings of the IEEE International Conference on Multimedia and Expo*, pages 622–627, 2019. 3
- [3] Zhao-Min Chen, Xiu-Shen Wei, Peng Wang, and Yanwen Guo. Multi-label image recognition with graph convolutional networks. In *Proceedings of the IEEE/CVF Conference on Computer Vision and Pattern Recognition*, pages 5177–5186, 2019. 3
- [4] Tat-Seng Chua, Jinhui Tang, Richang Hong, Haojie Li, Zhiping Luo, and Yan-Tao Zheng. Nus-wide: A real-world web image database from national university of singapore. In *Proceedings of ACM Conference on Image and Video Retrieval*, 2009. 6
- [5] Ekin Dogus Cubuk, Barret Zoph, Jonathon Shlens, and Quoc Le. Randaugment: Practical automated data augmentation with a reduced search space. In *Advances in Neural Information Processing Systems*, 2020. 7
- [6] Jia Deng, Wei Dong, Richard Socher, Li-Jia Li, Kai Li, and Li Fei-Fei. Imagenet: A large-scale hierarchical image database. In *Proceedings of the IEEE/CVF Conference on Computer Vision and Pattern Recognition*, 2009. 7, 11
- [7] Terrance Devries and Graham W. Taylor. Improved regularization of convolutional neural networks with cutout. *arXiv preprint arXiv:1708.04552*, 2017. 7
- [8] Xiaohan Ding, Xiangyu Zhang, Ningning Ma, Jungong Han, Guiguang Ding, and Jian Sun. Repvgg: Making vgg-style convnets great again. In *Proceedings of the IEEE/CVF Conference on Computer Vision and Pattern Recognition*, pages 13733–13742, 2021. 11
- [9] Mark Everingham, SM Eslami, Luc Van Gool, Christopher KI Williams, John Winn, and Andrew Zisserman. The pascal visual object classes challenge: A retrospective. *International Journal of Computer Vision*, pages 98–136, 2015. 6
- [10] Francois-Guillaume Fernandez. Torchcam: class activation explorer. <https://github.com/frgfm/torch-cam>, 2020. 12
- [11] Kaiming He, Xiangyu Zhang, Shaoqing Ren, and Jian Sun. Deep residual learning for image recognition. In *Proceedings of the IEEE/CVF Conference on Computer Vision and Pattern Recognition*, pages 770–778, 2016. 3, 11
- [12] Geoffrey Hinton, Oriol Vinyals, Jeff Dean, et al. Distilling the knowledge in a neural network. *arXiv preprint arXiv:1503.02531*, 2015. 2, 8
- [13] Peng-Tao Jiang, Chang-Bin Zhang, Qibin Hou, Ming-Ming Cheng, and Yunchao Wei. Layercam: Exploring hierarchical class activation maps for localization. *IEEE Transactions on Image Processing*, pages 5875–5888, 2021. 12
- [14] Diederik P Kingma and Jimmy Ba. Adam: A method for stochastic optimization. In *International Conference on Learning Representations*, 2015. 7
- [15] Jack Lanchantin, Tianlu Wang, Vicente Ordonez, and Yanjun Qi. General multi-label image classification with transformers. In *Proceedings of the IEEE/CVF Conference on Computer Vision and Pattern Recognition*, pages 16478–16488, 2021. 3
- [16] Tsung-Yi Lin, Michael Maire, Serge Belongie, James Hays, Pietro Perona, Deva Ramanan, Piotr Dollár, and C Lawrence Zitnick. Microsoft coco: Common objects in context. In *Proceedings of the European Conference on Computer Vision*, pages 740–755, 2014. 6
- [17] Shilong Liu, Lei Zhang, Xiao Yang, Hang Su, and Jun Zhu. Query2label: A simple transformer way to multi-label classification. *arXiv preprint arXiv:2107.10834*, 2021. 1, 3, 6
- [18] Yongcheng Liu, Lu Sheng, Jing Shao, Junjie Yan, Shiming Xiang, and Chunhong Pan. Multi-label image classification via knowledge distillation from weakly-supervised detection. In *Proceedings of the 26th ACM International Conference on Multimedia*, pages 700–708, 2018. 2, 3
- [19] Ze Liu, Yutong Lin, Yue Cao, Han Hu, Yixuan Wei, Zheng Zhang, Stephen Lin, and Baining Guo. Swin transformer: Hierarchical vision transformer using shifted windows. In *Proceedings of the IEEE/CVF International Conference on Computer Vision*, pages 10012–10022, 2021. 11
- [20] Ilya Loshchilov and Frank Hutter. Decoupled weight decay regularization. In *International Conference on Learning Representations*, 2018. 7
- [21] Roy Miles, Adrián López Rodríguez, and Krystian Mikolajczyk. Information theoretic representation distillation.

- arXiv preprint arXiv:2112.00459*, 2021. 3
- [22] Seyed Iman Mirzadeh, Mehrdad Farajtabar, Ang Li, Nir Levine, Akihiro Matsukawa, and Hassan Ghasemzadeh. Improved knowledge distillation via teacher assistant. In *Proceedings of the AAAI Conference on Artificial Intelligence*, pages 5191–5198, 2020. 2
- [23] Wonpyo Park, Dongju Kim, Yan Lu, and Minsu Cho. Relational knowledge distillation. In *Proceedings of the IEEE/CVF Conference on Computer Vision and Pattern Recognition*, pages 3967–3976, 2019. 2, 6
- [24] Nikolaos Passalis and Anastasios Tefas. Learning deep representations with probabilistic knowledge transfer. In *Proceedings of the European Conference on Computer Vision*, pages 268–284, 2018. 2, 6
- [25] Alec Radford, Jong Wook Kim, Chris Hallacy, Aditya Ramesh, Gabriel Goh, Sandhini Agarwal, Girish Sastry, Amanda Askell, Pamela Mishkin, Jack Clark, et al. Learning transferable visual models from natural language supervision. In *Proceedings of the International Conference on Machine Learning*, pages 8748–8763, 2021. 3
- [26] Tal Ridnik, Emanuel Ben-Baruch, Nadav Zamir, Asaf Noy, Itamar Friedman, Matan Protter, and Lihi Zelnik-Manor. Asymmetric loss for multi-label classification. In *Proceedings of the IEEE/CVF International Conference on Computer Vision*, pages 82–91, 2021. 3
- [27] Tal Ridnik, Gilad Sharir, Avi Ben-Cohen, Emanuel Ben-Baruch, and Asaf Noy. MI-decoder: Scalable and versatile classification head. *arXiv preprint arXiv:2111.12933*, 2021. 1, 3, 11
- [28] Adriana Romero, Nicolas Ballas, Samira Ebrahimi Kahou, Antoine Chassang, Carlo Gatta, and Yoshua Bengio. Fitnets: Hints for thin deep nets. *arXiv preprint arXiv:1412.6550*, 2014. 2
- [29] Mark Sandler, Andrew Howard, Menglong Zhu, Andrey Zhmoginov, and Liang-Chieh Chen. Mobilenetv2: Inverted residuals and linear bottlenecks. In *Proceedings of the IEEE/CVF Conference on Computer Vision and Pattern Recognition*, pages 4510–4520, 2018. 11
- [30] Liangchen Song, Jialian Wu, Ming Yang, Qian Zhang, Yuan Li, and Junsong Yuan. Handling difficult labels for multi-label image classification via uncertainty distillation. In *Proceedings of the 29th ACM International Conference on Multimedia*, pages 2410–2419, 2021. 2, 3, 7
- [31] Feng Sun, Ming-Kun Xie, and Sheng-Jun Huang. A deep model for partial multi-label image classification with curriculum based disambiguation. *arXiv preprint arXiv:2207.02410*, 2022. 6
- [32] Zhiyuan Tang, Dong Wang, and Zhiyong Zhang. Recurrent neural network training with dark knowledge transfer. In *Proceedings of the IEEE international Conference on Acoustics, Speech and Signal Processing*, 2016. 1
- [33] Yonglong Tian, Dilip Krishnan, and Phillip Isola. Contrastive representation distillation. In *International Conference on Learning Representations*, 2019. 2, 11
- [34] Ashish Vaswani, Noam Shazeer, Niki Parmar, Jakob Uszkoreit, Llion Jones, Aidan N Gomez, Łukasz Kaiser, and Illia Polosukhin. Attention is all you need. In *Advances in Neural Information Processing Systems*, 2017. 11
- [35] Jiazhi Xu, Sheng Huang, Fengtao Zhou, Luwen Huangfu, Daniel Zeng, and Bo Liu. Boosting multi-label image classification with complementary parallel self-distillation. In *Proceedings of the Thirty-First International Joint Conference on Artificial Intelligence*, 2022. 2, 3, 7
- [36] Shichao Xu, Yikang Li, Jenhao Hsiao, Chiuman Ho, and Zhu Qi. A dual modality approach for (zero-shot) multi-label classification. *arXiv preprint arXiv:2208.09562*, 2022. 3
- [37] Li Yuan, Francis EH Tay, Guilin Li, Tao Wang, and Jiashi Feng. Revisiting knowledge distillation via label smoothing regularization. In *Proceedings of the IEEE/CVF Conference on Computer Vision and Pattern Recognition*, 2020. 11
- [38] Sergey Zagoruyko and Nikos Komodakis. Paying more attention to attention: Improving the performance of convolutional neural networks via attention transfer. *arXiv preprint arXiv:1612.03928*, 2016. 2
- [39] Sergey Zagoruyko and Nikos Komodakis. Wide residual networks. In *Proceedings of the British Machine Vision Conference*, 2016. 11
- [40] Min-Ling Zhang and Zhi-Hua Zhou. A review on multi-label learning algorithms. *IEEE Transactions on Knowledge and Data Engineering*, pages 1819–1837, 2013. 1, 6
- [41] Ying Zhang, Tao Xiang, Timothy M Hospedales, and Huchuan Lu. Deep mutual learning. In *Proceedings of the IEEE/CVF Conference on Computer Vision and Pattern Recognition*, pages 4320–4328, 2018. 2
- [42] Borui Zhao, Quan Cui, Renjie Song, Yiyu Qiu, and Jiajun Liang. Decoupled knowledge distillation. In *Proceedings of the IEEE/CVF Conference on Computer Vision and Pattern Recognition*, pages 11953–11962, 2022. 2

## A. More Details of Implementation

In order to validate the proposed method with diverse architectures, we employ some commonly used models, including ResNet [11], Wide ResNet (WRN) [39], RepVGG [8], Swin Transformer [19], and MobileNet v2 [29]. For all the backbones, we utilize their pre-trained version on the ImageNet [6] as our base model.

For all experiments, similar to the previous work [27], we employ the label-wise embedding encoder consisting of a cross-attention module and a feed-forward fully-connected layer [34]. The cross-attention module takes full queries and feature maps as the input. We assign a query per class to ensure that each query corresponds to a single semantic. The multi-label classifier  $h(\cdot)$  is a fully-connected layer for each class, which outputs a predicted logit for a class label based on the input label-wise embedding.

## B. More Results on NUS-WIDE

Table 5 reports comparison results on NUS-WIDE with the same and different architectures of student and teacher models. For distillation between the same architectures, we choose a ResNet-101 [11] as the teacher and a ResNet-34 as the student. For distillation between different architectures, we choose a Swin-T [19] as the teacher and a MobileNet v2 [29] as the student. From the tables, it can be observed that the proposed L2D significantly outperforms all comparing methods, which convincingly validates the effectiveness of the proposed label-wise embeddings distillation.

Table 5. Results on NUS-WIDE validation.

Teacher	ResNet-101			Swin-T		
Student	ResNet-34			MobileNet v2		
Metrics	mAP	OF1	CF1	mAP	OF1	CF1
Teacher	55.32	75.56	61.31	59.73	77.30	65.44
Student	53.41	75.10	60.08	54.49	75.72	61.74
RKD	53.62	75.20	59.91	54.76	75.69	61.74
PKT	53.55	75.08	60.35	54.59	75.69	61.74
ReviewKD	53.52	75.23	60.44	54.85	75.84	61.75
MSE	53.52	75.13	59.94	54.86	75.80	61.69
PS	54.14	75.43	60.79	55.18	75.91	62.35
MLD	54.44	75.36	60.73	55.36	76.00	62.52
L2D	<b>55.31</b>	<b>76.17</b>	<b>62.79</b>	<b>56.91</b>	<b>76.92</b>	<b>63.89</b>

## C. More Results on Pascal VOC 2007

Table 7 and Table 8 report comparison results on Pascal VOC 2007 with the same and different architectures of student and teacher models. From the tables, it can be observed that the proposed L2D significantly outperforms all comparing methods, which convincingly validates the effectiveness of the proposed label-wise embeddings distillation. Compared with the results on MS-COCO, the perfor-

mance gap between L2D and comparing methods seems to become smaller. One possible reason is that VOC only contains about 1.5 labels per image, which leads conventional KD methods to obtain a better performance.

## D. Reversed Knowledge Distillation

In practice, teacher networks are always pretrained without any knowledge of the students architecture, which makes it possible that the student is more complicated than the teacher. Previous study [37] proved that the superior network can also be enhanced by learning from a weak network. To explore the performance of our method in this setting, we further conduct experiments on MS-COCO. In detail, we use a ResNet-34 as the teacher and a ResNet-101 as the student, which makes the vanilla student model outperforms the teacher. From Table 6, we can find that our method still outperforms all the other methods. This implies that our method is also effective for the reversed KD setting.

Table 6. Results of reversed knowledge distillation on MS-COCO validation, where the backbones of teacher and student model are respectively ResNet-34 and ResNet-101. The numbers in the brackets indicate the performance gaps between the student and the teacher.

Metrics	mAP	OF1	CF1
Teacher	70.19	72.30	66.50
Student	73.98 (+3.79)	75.01 (+2.71)	70.12 (+3.62)
RKD	74.03 (+3.84)	74.96 (+2.66)	70.01 (+3.51)
PKT	73.95 (+3.76)	74.94 (+2.64)	69.98 (+3.48)
ReviewKD	74.02 (+3.83)	74.96 (+2.66)	70.07 (+3.57)
MSE	74.21 (+4.02)	75.12 (+2.82)	70.18 (+3.68)
PS	74.70 (+4.51)	75.78 (+3.48)	71.08 (+4.58)
MLD	74.64 (+4.45)	75.78 (+3.48)	71.10 (+4.60)
L2D	<b>75.51(+5.32)</b>	<b>76.25(+3.95)</b>	<b>71.75(+5.25)</b>

## E. Parameter Sensitivity Analysis

In this section, we study the influence of balancing parameters  $\lambda_{MLD}$ ,  $\lambda_{CD}$  and  $\lambda_{ID}$  on the performance of L2D. A commonly used setting of the hyperparameter in vanilla KD that balances KL divergence against CE is 0.9 [33], which means the balancing parameter for CE is 0.1 and the one for KL divergence is 0.9. So we choose 10 for the balancing parameter for MLD, which is closest to the setting of vanilla KD. We set the balancing parameter for ID loss larger than CD loss considering that the ID loss may carry less information because there are only less than 3 labels for a instance on average, though it seems unnecessary since parameter sensitivity experiments in Figure 6 show that the performance of L2D are not sensitive to all of our balancing parameters.

## F. Visualization of Attention Maps

To further show the effectiveness of our proposed method L2D, we visualize some attention maps of the penultimate layer in the visual backbones using LayerCAM [13] implemented by Franois-Guillaume Fernandez [10]. We compare attention maps of the student model trained by L2D with some other methods in Figure 7 8 9. We compare L2D with: 1) Vanilla: student trained without distillation; 2) ReviewKD: a classical feature-based method which has the state-of-the-art performance among all conventional KD methods. In each figure, the first column shows the raw picture and the other columns show class activation maps overlaying on the raw picture. Each row represents a certain class. From these figures, we can find that L2D can locate the specified object more precisely than the other methods, which means it can not only pay attention to target objects, but also resist interference from similar but unrelated objects. All these comparisons show that L2D outperforms all comparing methods. It validates the effectiveness of our proposed label-wise embeddings distillation and shows great potential in MLKD.

Table 7. Results on Pascal VOC 2007 validation teacher and student models are in the **same** architectures.

Teacher	RepVGG-A2			ResNet-50			WRN-101			Swin-S		
Student	RepVGG-A0			ResNet-18			WRN-50			Swin-T		
Metrics	mAP	OF1	CF1									
Teacher	86.20	85.63	82.62	86.73	84.92	81.21	88.00	87.03	83.72	92.75	91.05	88.82
Student	83.79	83.36	79.83	84.01	83.60	79.42	88.52	87.21	84.08	91.31	89.98	88.00
RKD	83.75	83.41	79.85	84.48	83.54	79.83	88.21	87.33	84.55	91.52	90.44	88.51
PKT	83.63	83.53	80.04	84.12	83.10	79.31	87.69	87.07	84.14	91.28	90.17	88.03
ReviewKD	83.87	83.98	80.54	83.71	83.01	79.25	88.23	87.13	84.20	91.45	90.17	88.06
MSE	84.02	83.67	79.94	84.23	83.16	79.29	88.04	86.49	83.57	91.06	89.99	87.66
PS	83.77	83.74	80.28	84.44	83.78	79.95	88.30	86.92	83.91	91.21	90.25	88.12
MLD	83.65	83.66	80.02	84.48	84.07	80.29	88.29	87.16	84.25	91.43	90.72	88.81
L2D	<b>84.56</b>	<b>84.37</b>	<b>80.82</b>	<b>85.71</b>	<b>85.70</b>	<b>82.11</b>	<b>89.52</b>	<b>88.25</b>	<b>85.69</b>	<b>91.92</b>	<b>91.34</b>	<b>89.58</b>

Table 8. Results on Pascal VOC 2007 validation where teacher and student models are in the **different** architectures.

Teacher	ResNet-50			Swin-T			ResNet-50			Swin-T		
Student	RepVGG-A0			ResNet-18			MobileNet v2			MobileNet v2		
Metrics	mAP	OF1	CF1									
Teacher	86.73	84.92	81.21	91.43	89.81	87.63	86.73	84.92	81.21	91.43	89.81	87.63
Student	83.79	83.36	79.83	84.01	83.60	79.42	86.12	85.01	81.76	86.12	85.01	81.76
RKD	84.26	84.29	80.70	83.27	83.05	79.55	86.22	84.97	81.76	85.68	85.31	81.57
PKT	83.93	83.79	80.03	83.45	83.25	79.64	86.10	84.84	81.66	85.67	85.22	81.68
ReviewKD	84.07	83.62	80.34	83.37	83.08	78.93	85.87	85.04	81.73	85.69	85.10	81.56
MSE	84.01	84.05	80.52	83.60	83.06	79.46	86.20	84.94	81.84	85.80	85.51	81.98
PS	84.80	84.46	81.13	83.97	83.75	79.86	86.26	85.47	82.06	86.07	85.73	82.39
MLD	85.07	84.91	81.55	84.61	84.26	80.78	86.38	85.67	82.43	86.11	85.98	82.55
L2D	<b>86.26</b>	<b>85.85</b>	<b>82.55</b>	<b>85.87</b>	<b>85.67</b>	<b>82.17</b>	<b>87.32</b>	<b>86.48</b>	<b>83.26</b>	<b>87.37</b>	<b>86.88</b>	<b>83.68</b>

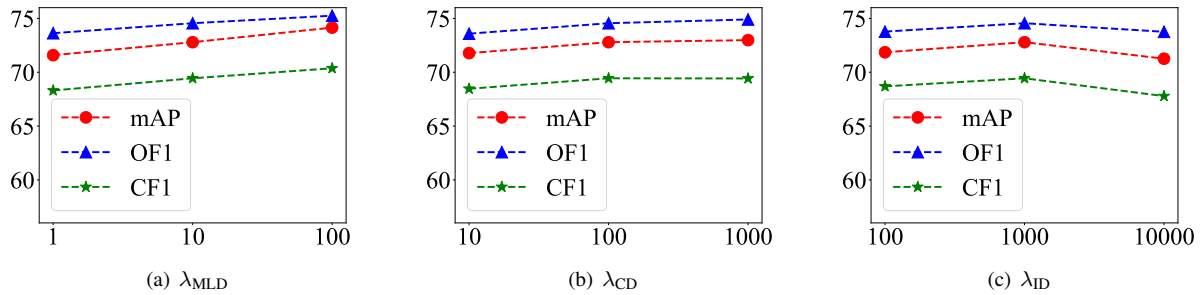
Figure 6. Student models' performance comparisons with different values of  $\lambda_{MLD}$ ,  $\lambda_{CD}$  and  $\lambda_{ID}$  respectively on MS-COCO with a ResNet-101 as the teacher and a ResNet-34 as the student.



Figure 7. An example of visualization of attention maps. We can find that on attention head for class *handbag*, both Vanilla and ReviewKD are interfered by some other objects and do not pay all attention to the handbag, but our L2D resists such interference successfully.

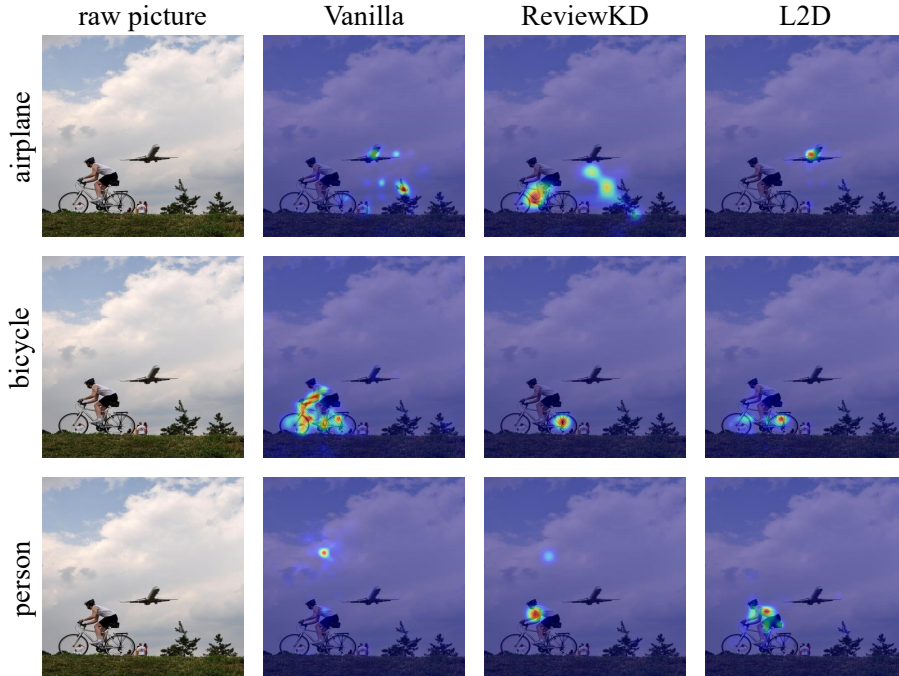


Figure 8. An example of visualization of attention maps. We can find that on attention head for class *airplane*, both Vanilla and ReviewKD do not pay all attention to the airplane: Vanilla is interfered by the plant and ReviewKD is interfered by the boy. But our L2D resists such interference successfully. On attention head for class *person*, both Vanilla and ReviewKD are interfered by the shades on the cloud, but L2D is not.

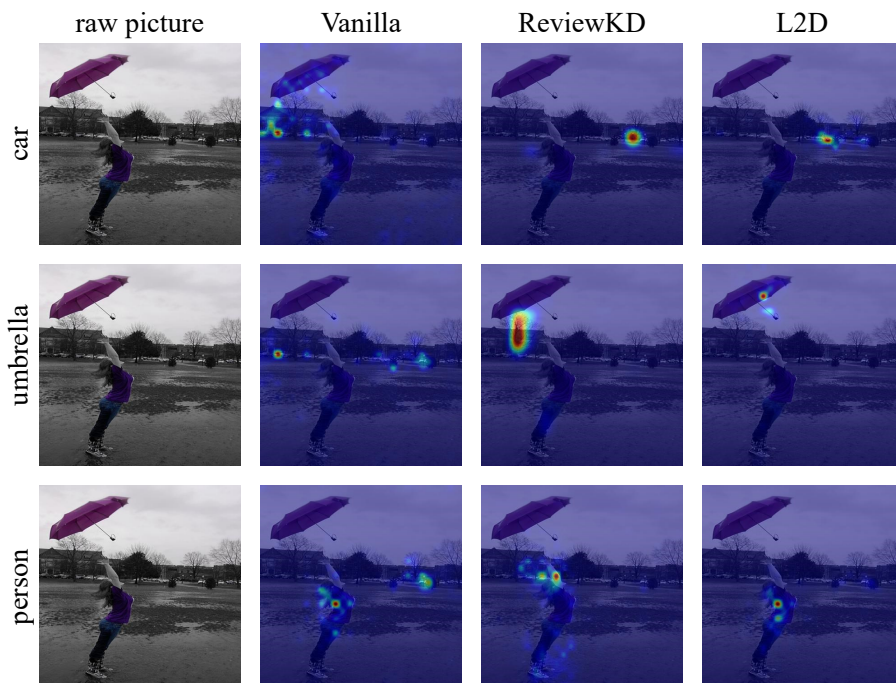


Figure 9. An example of visualization of attention maps. We can observe that on attention heads for class *car* and class *person*, Vanilla pays some of its attention to unrelated objects. On attention head for class *umbrella*, ReviewKD pays some of its attention to the house. Only L2D can concentrate on these three targets precisely.